IAI Journals.ASM.org

Colonization of Cecum Is Important for Development of Persistent Infection by *Yersinia pseudotuberculosis*

Anna Fahlgren,[a] Kemal Avican,[a,b] Linda Westermark,[a,b] Roland Nordfelth,[a] Maria Fällman[a,b]

Department of Molecular Biology, Umeå Centre for Microbial Research (UCMR), Umeå University, Umeå, Sweden[a]; Laboratory for Molecular Infection Medicine Sweden, Umeå University, Umeå, Sweden[b]

Yersiniosis is a human disease caused by the bacterium *Yersinia pseudotuberculosis* or *Yersinia enterocolitica*. The infection is usually resolved but can lead to postinfectious sequelae, including reactive arthritis and erythema nodosum. The commonly used *Yersinia* mouse infection model mimics acute infection in humans to some extent but leads to systemic infection and eventual death. Here, we analyzed sublethal infection doses of *Y. pseudotuberculosis* in mice in real time using bioluminescent imaging and found that infections using these lower doses result in extended periods of asymptomatic infections in a fraction of mice. In a search for the site for bacterial persistence, we found that the cecum was the primary colonization site and was the site where the organism resided during a 115-day infection period. Persistent infection was accompanied by sustained fecal shedding of cultivable bacteria. Cecal patches were identified as the primary site for cecal colonization during persistence. *Y. pseudotuberculosis* bacteria were present in inflammatory lesions, in localized foci, or as single cells and also in neutrophil exudates in the cecal lumen. The chronically colonized cecum may serve as a reservoir for dissemination of infection to extraintestinal sites, and a chronic inflammatory state may trigger the onset of postinfectious sequelae. This novel mouse model for bacterial persistence in cecum has potential as an investigative tool to unveil a deeper understanding of bacterial adaptation and host immune defense mechanisms during persistent infection.

Many bacterial pathogens that are responsible for a significant amount of human morbidity and mortality enter and leave the body through the digestive or respiratory tracts. Upon infection, activation of both innate and adaptive immune responses usually occurs. If the pathogen survives the innate immune reactions, the adaptive immune system is important for clearing the pathogen. Thus, the mode and efficiency of a bacterial infection depend on various factors, including the specific niche within the host, the growth rate of the pathogen, and its ability to circumvent initiation of various immune responses and/or efficiently evade the response.

Some pathogenic bacteria are capable of maintaining infection in mammalian hosts in the presence of an induced immune response, in some cases giving rise to persistent infection (1–3). Diagnosis of a persistent infection can be difficult, as signs are not always obvious. A prolonged persistent infection can cause a chronic inflammatory state, which could lead to complications or even precipitation of certain diseases in susceptible hosts (2–4). It may also cause organ damage, which eventually weakens the immune system, leading to symptomatic infection.

The enteropathogenic *Yersinia* species *Y. pseudotuberculosis* and *Y. enterocolitica* cause acute enteritis/gastroenteritis, mesenteric lymphadenitis, and diarrheal disease, characterized by fever and abdominal pain, which may resemble acute appendicitis (5, 6). The bacterium is ingested through contaminated food or water and localizes to the distal ileum and proximal colon. Current knowledge of enteropathogenic *Yersinia* infection is mainly based on studies using an oral mouse infection model with infection inocula that cause disease symptoms similar to those seen in affected humans. In mice, the bacteria colonize Peyer's patches (PPs) of the small intestine during passage through the digestive tract, and the chromosomally encoded protein invasin contributes to bacterial entry into the PPs by binding to β1 integrins, which are expressed on the apical side of the M cells in the follicle-associated epithelium (7–9). After invasion into the intestinal lamina propria, bacteria spread further to the mesenteric lymph nodes (MLN) and, possibly, to the spleen and liver. In addition, *Yersinia* has also been shown to disseminate directly from the intestine to the liver and spleen without transfer through the MLN (10).

Pathogenicity is mainly caused by an extrachromosomal 70-kb virulence plasmid encoding a type III secretion system (T3SS) and the virulence factors *Yersinia* outer proteins (Yops). Yops (YopE, YopH, YopM, YpkA, YopK, YopT, and YopJ/P) are powerful effector molecules that are delivered into host cells via the T3SS (11). The primary target cells for Yop delivery in PPs, MLN, and spleen are neutrophils, macrophages, and dendritic cells, underscoring the importance of disarming phagocytic cells early in infection (12). By delivery of virulence effectors into host cells, *Yersinia* hijacks the intracellular machinery to interfere with phagocytosis, signaling pathways that are involved in the regulation of the actin cytoskeleton, apoptosis, and the inflammatory response, thus favoring the survival of the bacteria (13–15).

While most cases of yersiniosis are mild and usually self-limited in immunocompetent humans, infection with enteric *Yersinia* may also lead to the development of a persistent infection

Received 21 March 2014 **Returned for modification** 16 April 2014
Accepted 28 May 2014
Published ahead of print 2 June 2014
Editor: A. J. Bäumler
Address correspondence to Anna Fahlgren, anna.fahlgren@molbiol.umu.se.
Supplemental material for this article may be found at http://dx.doi.org/10.1128/IAI.01793-14.

doi:10.1128/IAI.01793-14

with or without development of postinfectious sequelae, such as reactive arthritis (16). Persistence of enteric *Yersinia* has been reported in patients to last up to several years after the initial infection (5, 17, 18). Interestingly, there are many reported associations between infections by enteropathogenic *Yersinia* and development of Crohn's disease, inflammatory bowel disease, pseudoappendicitis, and reactive arthritis, pointing to a possible link between a persistent infection and clinical manifestations (16, 19).

As there is no mouse model for studies of persistent infection by *Yersinia*, it has been difficult to further explore the interesting correlations between persistent *Yersinia* infections and infectious sequelae and to study the immune response during these persistent infections. Since infection models in mice often depend on obvious signs of infection as readouts for the disease, most infection studies using mouse models involve high infection doses that give clear disease symptoms. In the case of enteric *Yersinia* infection in mice, disease signs are scored by the appearance of diarrhea, hunched back, fuzzy fur, and weight loss. In the present study, we explored infection caused by sublethal doses of *Y. pseudotuberculosis* in mice, using real-time bioluminescent imaging (BLI) of luciferase-expressing bacteria. We show that virulent *Y. pseudotuberculosis* can cause persistent infection in mice in which the bacteria reside in the cecum of asymptomatic mice and are shed into feces.

MATERIALS AND METHODS

Mice. Female BALB/c, C57BL/6, and FVB/N mice 8 to 9 weeks old (Taconic, Denmark and USA) were housed in accordance with the guidelines of the Swedish National Board for Laboratory Animals and used for infection experiments in accordance with the guidelines of the Animal Ethics Committee of Umeå University (Dnr A104-08 and A108-10). Mice were allowed to acclimatize to the new environment for 1 week before the experiments.

Bacterial strains. Bioluminescent *Yersinia pseudotuberculosis* Xen4 (Caliper Life Science), based on the wild-type (wt) isolate YPIII with the *luxCDABE* operon from *Photorhabdus luminescens* integrated on the virulence plasmid [here denoted YPIII(pIBX)], was used for infection in mice. Bioluminescent *yop* mutant strains for *yopH* [YPIII(pIBX30)] (20), *yopE* [YPIII(pIBX526)] (21), *yopHE* [YPIII(pIBX526-30)] (this study), and *yopJ* [YPIII(pIBX240)] (this study) were created in Xen4 by amplifying DNA fragments flanking the genes to be deleted. A secondary PCR was performed using the flanking-region products as the templates; the resulting fragments were cloned into the suicide vector pDM4 (21) and were then introduced into the YPIII(pIBX) strain by conjugational mating using *Escherichia coli* S17-1 *pir* as the donor strain. To create the double mutant *yopHE* strain [YPIII(pIBX526-30)], pDM4 containing the DNA flanking regions for deletion of *yopH* was introduced into the YPIII(pIBX526) strain by conjugation, as above. For selection of appropriate homologous recombination events, established methods were used (21). All mutants were confirmed by sequencing.

Mouse infection. Prior to infection, mice were deprived of water and food for 16 h and then allowed to drink bacterium-containing water for 6 h. Bacteria were subcultured on Luria broth (LB) agar plates, supplemented with kanamycin (50 μg/ml). For infection, the bacteria were grown in LB overnight at 26°C. Bacterial concentrations were estimated by optical density (OD) at 600 nm. Cultures were collected, centrifuged, and resuspended to 10^6 to 10^8 CFU/ml in sterilized tap water, supplemented with 150 mM NaCl.

The infection dose was determined by viable count combined with drinking volume measurements through weighing of the bacteria containing water before and after infection and divided by the number of mice in each case. Mice were inspected frequently for clinical signs to characterize their response to *Y. pseudotuberculosis* and to ensure that infected mice showing prominent clinical signs, including inactivity, lack of responsiveness to stimulation, reduced eating or drinking, hunched posture, ruffled fur, soft feces or diarrhea, dehydration, and weight loss, were euthanized promptly to prevent suffering. In some experiments, mouse-tail blood was collected prior to anesthesia and immediately analyzed for hemoglobin (Hb) levels, using a HemoCue reader and cuvettes (HemoCue AB, Ängelholm, Sweden), as well as blood glucose levels, using the GlucoSurePlus system (HaeMedic AB, Sweden). The body weights of all of the mice were monitored throughout the experiments.

Real-time imaging of bioluminescence. Prior to imaging, mice were anesthetized using the XGI-8 gas anesthesia system (Caliper Life Science), which allows control over the duration of anesthesia. Oxygen mixed with 2.5% IsoFloVet (Orion Pharma, Abbott Laboratories Ltd., Great Britain) was used for initial anesthesia, and 0.5% isoflurane in oxygen was used during imaging. To analyze bacterial localization within organs, mice were euthanized, and the intestine, MLN, liver, and spleen were removed and imaged by BLI.

CFU assays. For analyses of bacterial colonization, viable count measurements were made from infected mouse tissues after homogenization using a Dispomix drive homogenizer (Medic Tools, Switzerland). Serial dilutions of the homogenates were plated on LB agar plates, supplemented with kanamycin (50 μg/ml). Colonies were counted after 48 h of incubation at 26°C. The variability of *Y. pseudotuberculosis* tissue infections rendered the resulting data nonparametric.

Quantification of bioluminescence. Acquisition and analysis of the bioluminescence from the *Yersinia* strains in the live mice were performed using Living Image software, version 3.1 (Caliper Life Sciences). Total photon emission was collected and compared between groups by applying a common scale. For emission of photons within a specific region, photon flux (photons/s/cm^2/steradian) was measured by using the region of interest (ROI) tool. Background signals were quantified similarly, using ROIs of samples, which were not spiked with the bioluminescent bacteria.

Immunohistochemistry. Tissues were harvested from uninfected and infected mice, rinsed in phosphate-buffered solution (PBS) to remove any fecal matter, frozen on isopentane, prechilled in liquid nitrogen, and stored at −80°C. For immunohistochemical staining, 10-μm cryosections were fixed in 4% paraformaldehyde (PFA), and free aldehyde groups were blocked in 0.1 M glycine for 10 min. Endogenous peroxidases were blocked in PBS, 2 mM NaN_3, 0.03% H_2O_2 at 37°C, and endogenous biotin was blocked with avidin-biotin treatment (Vector Laboratories). The sections were incubated in 0.1% bovine serum albumin (BSA; Boehringer Mannheim) with the following antibodies: hamster anti-mouse CD11c (clone N418; AbD Serotec); rat anti-mouse Ly6G (clone 1A8; BD Biosciences Pharmingen); rat anti-mouse Ly6C/6G (clone RB6-8C5; BD Biosciences Pharmingen); rat anti-mouse F4/80 (clone CI:A3-1; AbD Serotec). Armenian hamster IgG (Serotec) and rat IgG2b (Serotec) were used as isotype controls. A biotinylated secondary antibody, biotinylated goat anti-Armenian hamster (Jackson ImmunoResearch) or biotinylated mouse anti-rat (Jackson ImmunoResearch), was applied; the signal was amplified with the Vectastain ABC enhancement kit (Vector Laboratories Inc., Burlingame, CA, USA) and developed with 3,3′-diaminobenzidine (Fast DAB tablet sets; Sigma). Finally, the tissue sections were stained with methyl green (Sigma) and mounted in Canada balsam (Sigma). PFA-fixed cryosections were incubated in 0.5% toluidine blue in 20% ethanol to reveal gross tissue histology. After treatment, the sections were dehydrated in ethanol (70%, 95%, and 95%), washed in xylene, and mounted in Canada balsam. The stained sections were examined using a Nikon 90i microscope, and images were captured using a Nikon DSFi1 camera with Nis-Elements AR software.

Luminex multiplexing. Serum samples from mice were analyzed for the presence of 11 mouse cytokines by multiplexing. Blood was sampled from the tail vein of mice, allowed to clot for 30 min, and centrifuged at 10,000 × *g* for 10 min at +4°C, and the cell-free serum was transferred to clean tubes for storage at −80°C until analysis. Concentrations of interleukin-1β (IL-1β), IL-4, IL-10, IL-12p70 subunit, IL-15, IL-17, IL-18,

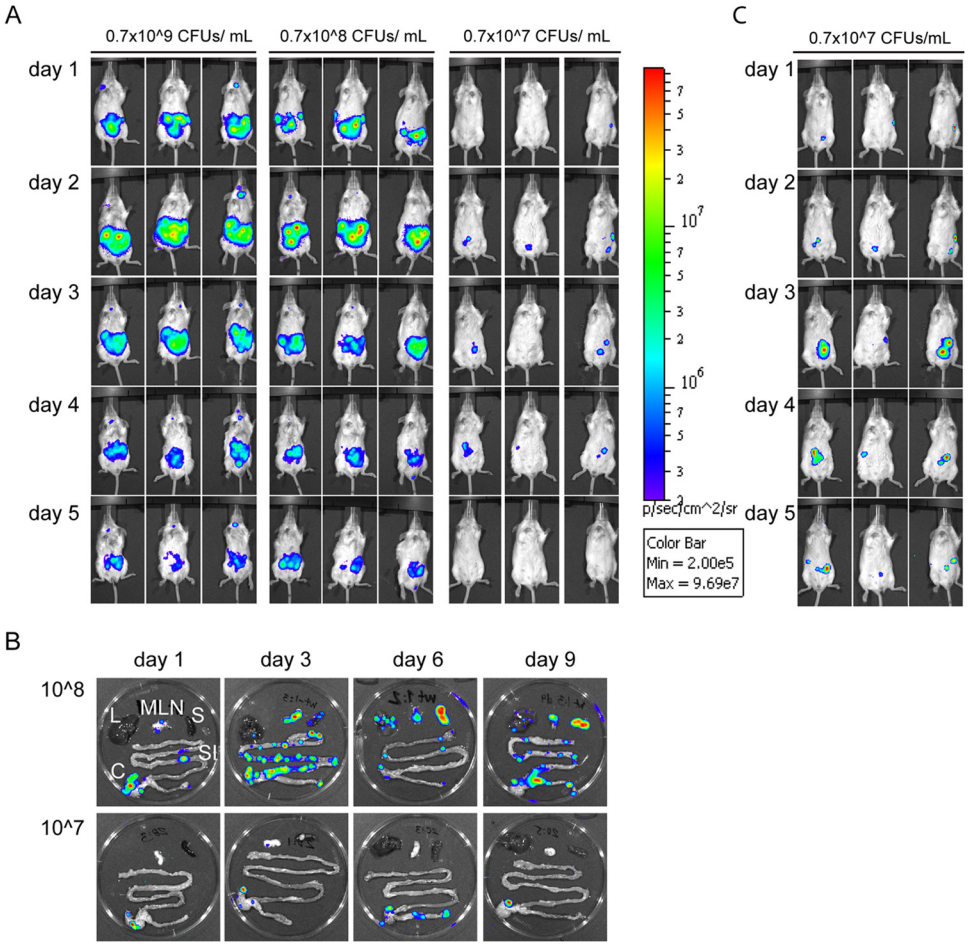

FIG 1 Real-time monitoring of *Y. pseudotuberculosis* infection, using IVIS. (A) Mice were infected orally with 0.7×10^9, 0.7×10^8, or 0.7×10^7 CFU/ml of overnight cultures of bacteria. The process of infection was monitored every day p.i. by detecting total photon emission, using the IVIS Spectrum system. The intensity of bioluminescent emission is represented as pseudocolors with variations in color representing light intensity; red represents the most intense light emission, while blue corresponds to the weakest signal. A common sensitivity scale is used for the different doses. (B) Spread of infection in organs during high-dose infection. SI, small intestine; C, cecum; MLN, mesenteric lymph nodes; S, spleen; L, liver. (C) Analysis of mice infected with 0.7×10^7 CFU/ml (same mice as in panel A) on an individual scale for each image, allowing for detection of low signals.

IL-23, gamma interferon (IFN-γ), KC, and tumor necrosis factor alpha (TNF-α) were analyzed using a Luminex-based multiplex cytometric bead array kit (Bio-Plex Pro cytokine assay; Bio-Rad). Individual samples were run in duplicate, using the Bio-Plex 200 System, and analyzed by Bio-Plex Manager 6.0 software.

Statistics. Data from the *in vivo* imaging system (IVIS) analyses and multiplex array were analyzed using GraphPad Prism version 5. Differences were analyzed by Student's unpaired *t* test or the Mann-Whitney nonparametric test with significance set at $P < 0.05$ (*), $P < 0.01$ (**), or $P < 0.001$ (***). Error bars in graphs correspond to the standard errors of the means.

RESULTS

***Y. pseudotuberculosis* infection in mice in real time.** Our understanding of the progression of bacterial infections in mouse models is primarily based on observations of single events in individual mice. These traditional mouse infection studies require mice to be euthanized at different time points for determination of bacterial counts and localization. With the aim to follow the progress of *Y. pseudotuberculosis* infection *in vivo* within the same group of animals, we employed BLI using an *in vivo* imaging system, IVIS Spectrum, for real-time detection of bacteria in mice.

BLI is based on the detection of visible light that is produced by luciferase-catalyzed reactions and has emerged as a valuable tool for noninvasive studies of infection in small laboratory animals, as it allows for detection and semiquantification of bacteria and visual characterization of the infection within intact mice (22). For infections, we used the bioluminescent wild-type *Y. pseudotuberculosis* strain YPIII(pIBX). BALB/c mice were orally infected with 10^7 to 10^9 CFU/ml, and progress of infection was monitored over time by *in vivo* imaging of anesthetized mice, in combination with imaging of dissected organs from mice sacrificed at different time points postinfection (p.i.) to reveal bacterial localization. The infected mice were also visually inspected for signs of disease.

Initially, the bioluminescent signals appeared in the lower abdomen (Fig. 1A). In severely affected mice (infection doses, 10^8 to 10^9 CFU/ml), the bioluminescent signals moved with time to the upper right side (corresponding to the spleen) and then finally to the upper left side (corresponding to the liver). These results correlated well with the visual inspections, where mice infected with 10^8 and 10^9 CFU/ml started to show external signs of infection, such as ruffled fur and soft feces or diarrhea, from day 3 p.i.

In the following days, infected mice showed increased hunched posture, dehydration, and weight loss. Mice that had an infectious dose of 10^9 or 10^8 CFU/ml were terminally sick by days 5 to 7 or 7 to 10 p.i., respectively, whereas mice infected with 10^7 CFU/ml did not appear to be affected by the infection at these time points. BLI analyses of dissected organs from mice infected with 10^8 CFU/ml revealed that the main bulk of bacteria were in discrete areas in the cecum, but also in PPs, and occasionally in MLN at 24 h p.i. (Fig. 1B, upper panel). From day 3 p.i., bacteria were found in the MLN and, in some cases, the spleen and liver, indicating systemic spread. In accordance, mice that had to be euthanized due to signs of progressive disease were strongly affected with small empty ceca, blood-filled mesenterium, enlarged PPs, empty stomach, necrotic spleen and liver, and occasional liver abscesses; in these mice, bacteria were detected in MLN, liver, and spleen. According to the BLI analysis, mice infected with the lower dose (10^7 CFU/ml) were also colonized during the time of infection. The levels of total flux were lower than those in mice infected with the higher doses (Fig. 1A), but separate analyses on an individual scale showed bioluminescent signals in the lower abdominal tract in a fraction of the mice (Fig. 1C). None of these mice showed any signs of disease, and analyses of dissected organs revealed bacterial bioluminescence in the cecum from the onset of infection, as well as at days 6 to 12 p.i. (Fig. 1B, lower panel, and data not shown).

Taken together, analyses of mice infected with different doses revealed that *Y. pseudotuberculosis* mainly infects the cecum and PPs initially, and thereafter, depending on infection dose, bacteria can spread systemically, causing severe disease. In contrast to high-infection doses that result in disease signs and systemic spread, low-dose infections result in bacterial colonization in the cecum that remains even at later time points, without signs of disease.

Low-dose infection results in persistent infection. Given that the mice that were infected at low doses appeared to be asymptomatic and yet carried the bacteria in the cecum, we employed additional low-dose infection experiments, whereupon mice were followed for a prolonged period of time. First, infectious doses of 10^7 and 10^6 CFU/ml were given to BALB/c mice, and the infection was followed for 24 days. In this experiment, 30 out of 30 mice were initially infected by a dose of 10^7 CFU/ml, and 16 out of 30 mice were infected by 10^6 CFU/ml. Using these low doses for infection, three types of scenarios were obvious: acute infection, clearance, or a carrier state, showing no signs of infection (here termed asymptomatic infection). While the majority of the infected mice remained apparently asymptomatic, some showed signs of disease from day 3 to day 11 p.i., at which time some developed severe/terminal disease (6/30 for 10^7 CFU/ml, 6/16 for 10^6 CFU/ml). This result correlated with the BLI analysis of these mice, which showed a progressive spread of bioluminescent bacteria from the lower abdomen to MLN, spleen, and liver, confirmed by dissection of organs. Mice that survived the acute phase of infection (asymptomatic or slightly symptomatic) either cleared infection at different time points, starting at day 7 p.i., or remained infected (Fig. 2A).

At day 24 p.i., more than 10% of the mice that were infected with low doses still showed a bioluminescent signal in the lower part of the abdomen (3/30 for 10^7 CFU/ml and 2/16 for 10^6 CFU/ml). Dissections followed by IVIS analysis at this time point revealed that the sources of bacterial signals were discrete areas in the cecum (Fig. 2B). Bioluminescence was measured using specified regions of interest (ROIs) to determine total flux emitted from the abdomen of each mouse. Although the infection dose of 10^7 CFU/ml gave a higher total flux emitted early in infection, the two infection doses showed similar total flux values emitted from infected mice from day 7 p.i. (Fig. 2C).

The asymptomatic carriage of *Y. pseudotuberculosis* in the cecum suggested potential bacterial persistence. Therefore, we performed seven additional infection experiments, including, in total, 120 BALB/c mice that received an infectious dose of 10^7 CFU/ml, where BLI analyses, determination of bacterial counts, and general disease assessments were employed. To determine the initial bacterial colonization in different organs, groups of five mice were sacrificed on days 1, 3, and 7 p.i. The dissected tissues were analyzed with BLI to determine the presence of bacteria, and subsequently, the small intestine, large intestine, cecum, MLN, spleen, and liver were homogenized and plated on selective plates. This analysis showed that the cecum was the main colonization site at these early time points (see Fig. S1A in the supplemental material). These additional infection experiments confirmed the previous finding that, upon infection with a sublethal dose, some mice succumbed to infection between days 7 and 24 p.i., while the remaining mice either cleared the infection or remained infected (Fig. 2D). Importantly, a signal could not be detected in the dissected organs from mice that were considered to have cleared the infection, as determined by the IVIS analysis of the live animal, and fecal pellets, which were homogenized after clearance of the signal, were negative for growth of *Yersinia*. Consistent with previous findings, dissections of organs from infected but asymptomatic mice at later time points always showed bacteria confined to the cecum and, in rare cases, PPs, with no signs of general organ defects caused by the pathogen (see Fig. S1B in the supplemental material). Homogenization from a luminescence-positive cecum on day 24 revealed 1.3×10^6 CFU. Although the portion of infected, asymptomatic BALB/c mice decreased with time, this phenomenon was evident for a surprisingly long time, up to 51 days when the experiment was terminated (Fig. 2D; Table 1).

Hence, upon infection of BALB/c mice with sublethal infection doses of *Y. pseudotuberculosis*, a fraction of mice contained bacteria for $\geq$51 days in the cecum without resulting in systemic spread. We suggest that the observed long-lasting infection in asymptomatic mice reflects persistent infection.

***Y. pseudotuberculosis* persistence requires YopH and YopE.** Type III secretion is required for survival of *Y. pseudotuberculosis* in the cecum and PPs during high-dose infections (23), where YopH is important for the spread to the MLN and YopE is important for dissemination from the MLN (24). We next asked if these antiphagocytic effectors as well as another Yop effector, YopJ, are required for persistence in cecum. The serine/threonine acetyltransferase YopJ induces cell death, resulting in proinflammatory cytokine processing as well as increased intestinal permeability (25, 26), and was therefore interesting to include in a low-dose experiment.

BALB/c mice were infected with 10^7 CFU/ml of wt ($n = 14$) or *yopH*, *yopE*, or *yopJ* mutants ($n = 9$ for each strain) or with 10^8 CFU/ml of the *yopHE* ($n = 8$) double mutant and monitored by BLI. The higher dose was employed for the double mutant to reveal if a high infection dose would allow asymptomatic persistence of this mutant strain, which is highly attenuated in its ability to cause severe infection (24). None of the mice that were infected with the *yopH* or *yopE* mutants showed any sign of disease, and

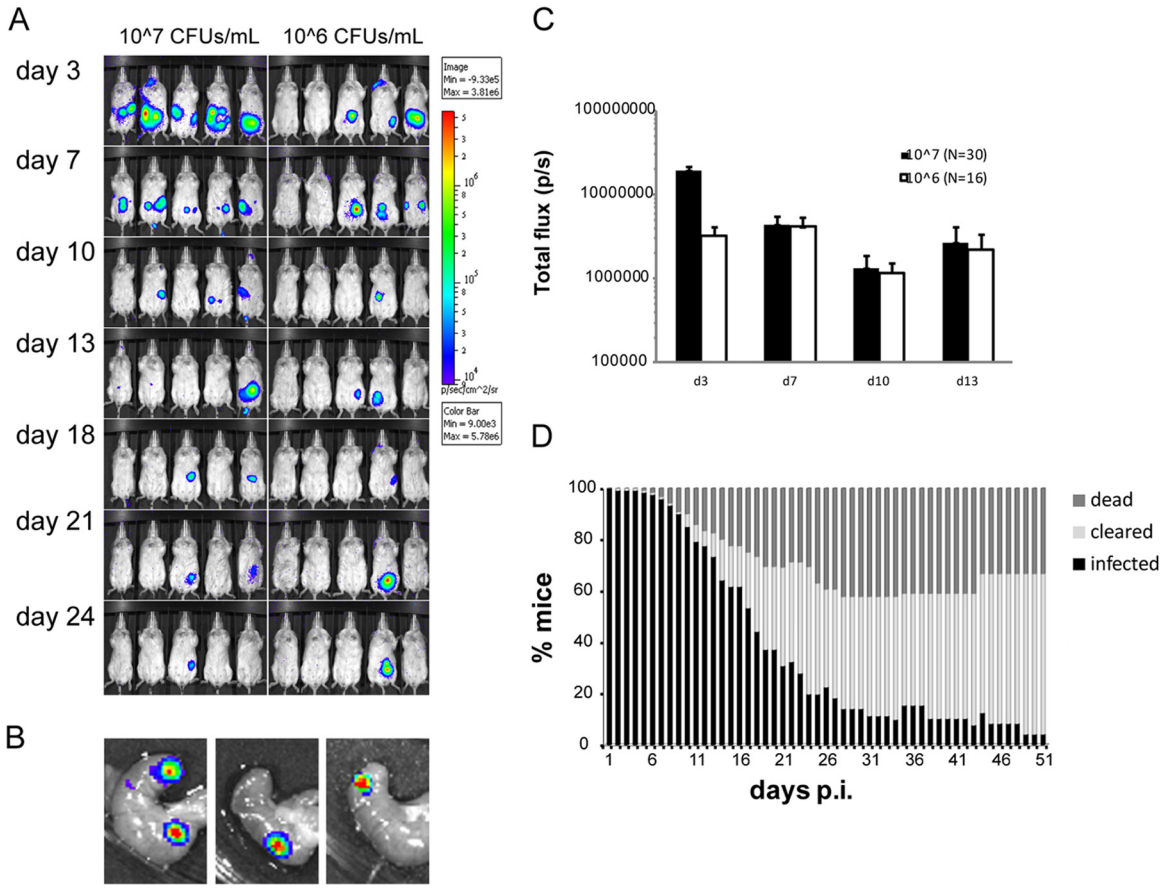

FIG 2 Low-dose infection results in asymptomatic infection with localization in the cecum. (A) IVIS analysis of BALB/c mice infected with 10^6 or 10^7 CFU/ml in the drinking water. The figure shows representative groups from each infection dose. The intensity of bioluminescent emission is represented as pseudocolors with variations in color representing light intensity; red represents the most intense light emission, while blue corresponds to the weakest signal. A common sensitivity scale is used for the different doses. (B) IVIS analysis of ceca dissected from asymptomatic mice infected with *Y. pseudotuberculosis* on day 24 p.i. (C) Total flux (photons/s) in a defined region of interest of IVIS images from infected mice. Data are presented as means ± standard errors of the means. (D) Results of low-dose infection of *Y. pseudotuberculosis* in BALB/c (seven experiments, $n = 120$), showing the percentage of infected mice that succumbed to infection (dark gray), cleared infection (light gray), or maintained infection (black). Mice were defined as cleared or infected based on IVIS analyses. Note that the panel summarizes several independent infection experiments with different scheduled termination points that affect the total number of mice included in the calculation.

they did not succumb to infection, although all showed bioluminescent activity by bacteria, whereas infection with the *yopJ* mutant resembled that of the wt strain (Fig. 3A; see also Fig. S2A in the supplemental material). The signals were clearly lower in mice that were infected with *yopH* or *yopE* mutants, in comparison to those in mice that were infected with wt or the *yopJ* mutant, and remained in the same region of the gut until bacterial clearance, which occurred earlier: day 15 for the *yopH* mutant, day 18 for the *yopE* mutant, day 28 for the wt, and day 25 for the *yopJ* mutant (Fig. 3B). Organ dissections showed that all single *yop* mutants colonized the cecum at both days 3 and 7 p.i., while *yopH* mutants never, and *yopE* mutants only rarely, were found in other organs at the later time point (Fig. 3C). Mice infected with a 10-times-higher concentration of the double *yopHE* mutant showed very weak initial BLI signals in 2/12 mice on day 1 p.i.; these signals were lost by day 3. Organs that were analyzed from day 1 revealed no bacterial signals from the *yopHE* mutant-infected mice (see Fig. S2B in the supplemental material). Taken together, these data indicate that YopH and YopE together contribute to persistence, likely by enabling efficient initial colonization in cecum.

TABLE 1 Bioluminescent signals detected *in vivo* differ between mouse strains

Day p.i.	% of mice (no. of mice analyzed) by strain and dose[a]:			
	C57BL/6		BALB/c	FVB/N
	10^7 CFU/ml	10^8 CFU/ml	(10^7 CFU/ml)	(10^7 CFU/ml)
14	31 (26)	45 (111)	64 (120)	71 (112)
21	7.7 (26)	9.0 (111)	31 (120)	55 (112)
24		7.7 (65)	20 (111)	46 (112)
42			10 (39)	25 (79)
51			4.2 (24)	18 (33)

[a] Percentage of mice in which bioluminescent signals were detected by IVIS out of total infected mice.

FVB/N mice are most suitable for studying asymptomatic persistence of *Y. pseudotuberculosis*. To determine if the observed cecal localization during an asymptomatic, persistent infection of *Y. pseudotuberculosis* in mice can be generalizable to

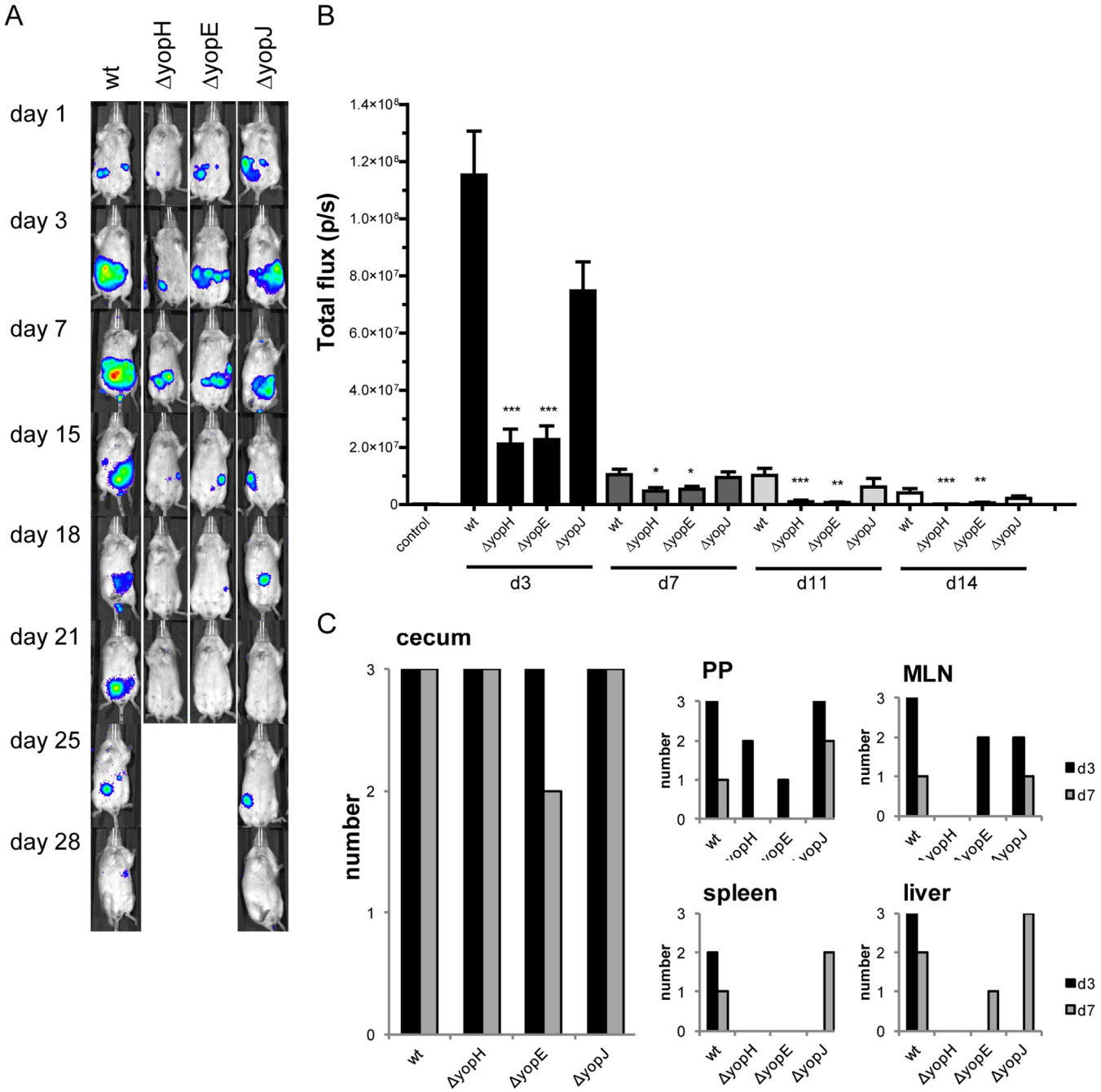

FIG 3 *Y. pseudotuberculosis* persistence requires YopH and YopE. BALB/c mice were infected with 1.4×10^7 CFU/ml of wt *Y. pseudotuberculosis* or 1.4×10^7 CFU/ml of *yopH* (ΔyopH), 1.8×10^7 CFU/ml of *yopE* (ΔyopE), or 1.7×10^7 CFU/ml of *yopJ* (ΔyopJ) bacteria. (A) IVIS analysis, showing images of mice that were colonized by bacteria. The intensity of bioluminescent emission is represented as pseudocolors with variations in color representing light intensity; red represents the most intense light emission, while blue corresponds to the weakest signal. (B) Total flux (photons/s) measured in a defined region of interest over the mouse abdomen. Data are presented as means ± standard errors of the means. Significance compared to the wt was analyzed using the Mann-Whitney test, with significance set at $P < 0.05$ (*), $P < 0.01$ (**), and $P < 0.001$ (***). (C) Bacterial bioluminescence in organs that were dissected from infected mice on days 3 and 7 p.i. ($n = 3$ from each bacterial strain).

other strains of mice, C57BL/6, FVB/N, and BALB/c mice were infected with 10^7 CFU/ml in parallel. BLI analysis on day 3 showed that 10/15 C57BL/6 mice, 14/15 BALB/c mice, and 13/15 FVB/N mice were initially colonized, and organ analysis on day 7 p.i. revealed bacterial localization in the ceca of all three mouse strains (see Fig. S3A in the supplemental material). In C57BL/6 mice, the bioluminescent bacterial signals were maintained only until day 21 p.i. (1/10). At this time point, 7/14 BALB/c mice and 9/13 FVB/N mice maintained bacteria. The C57BL/6 mice were obviously more resistant to infection than were the BALB/c and FVN/N mice, with lower initial infection efficiency, lower susceptibility to systemic spread, and faster clearance of bacteria, which

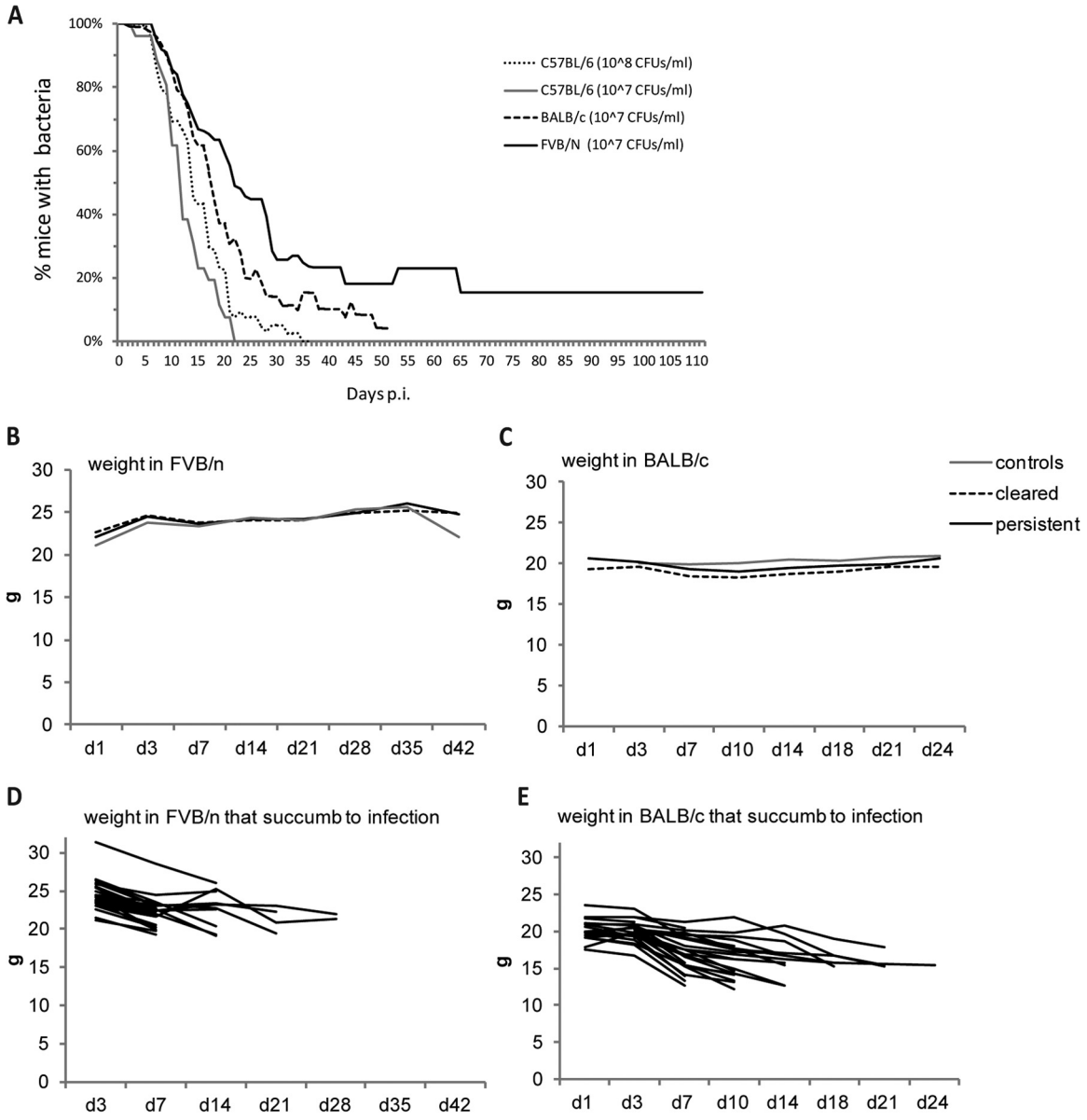

FIG 4 Persistence in different mouse strains. (A) Persistence of *Y. pseudotuberculosis* infection in different mouse strains infected with 10^7 CFU/ml: C57BL/6 (three experiments, $n = 26$), BALB/c (seven experiments, $n = 120$), and FVB/N (seven experiments, $n = 112$). IVIS imaging was employed to determine if mice were infected at each time point. (B and C) Weight curves of FVB/N (B) and BALC/c (C) control mice or mice infected with 10^7 CFU/ml of *Y. pseudotuberculosis*. Gray line, control mice (BALB/c, $n = 7$; FVB/N, $n = 13$); black line, persistent mice (BALB/c, $n = 13$; FVB/N, $n = 11$); black dashed line, cleared mice (BALB/c, $n = 46$; FVB/N, $n = 22$). (D and E) Weight curves of FVB/N (D) ($n = 28$) and BALC/c (E) ($n = 29$) mice infected with 10^7 CFU/ml of *Y. pseudotuberculosis* that succumbed to infection.

were completely eliminated after 21 days. Consistent with previous experiments, the last BALB/c mouse with a bioluminescent signal was detected on day 48 p.i. Interestingly, FVB/N mice showed bacterial signals from the lower abdomen up to 115 days p.i. in 2 out of 13 mice. When several infection experiments with C57BL/6 (three experiments, $n = 26$), BALB/c (seven experiments, $n = 120$), and FVB/N (seven experiments, $n = 112$) mice were compared, it was evident that FVB/N and BALB/c mice showed similar initial infection frequencies and total bioluminescent signals, as well as similar susceptibilities to systemic spread and death (Fig. 4A; see Fig. S3B in the supplemental material). There was, however, a striking difference in the number of persistently infected mice, which was more than 2-fold higher for FVB/N mice (Table 1).

Although mice with persistent infections appeared asymptomatic, their general health parameters were measured, such as weight, hemoglobin, and blood glucose levels. Weight changes of infected, asymptomatic mice (BALB/c and FVB/N) did not differ from those of uninfected control mice (Fig. 4B and C). It was obvious, though, that the mice which succumbed to infection dramatically lost weight, starting from the onset of disease signs (Fig. 4D and E). Neither blood glucose levels (mean values, 9.6 ± 0.93 mM/liter in FVB/N mice, $n = 6$, and 6.9 ± 0.31 mM/liter, in BALB/c mice, $n = 13$) nor hemoglobin levels (mean value, 143 ±

2.05 g/liter in FVB/N mice, $n = 6$, and 175 ± 4.37 g/liter in BALB/c mice, $n = 13$) dropped in association with persistence, whereas they both showed a dramatic drop for terminally sick mice (data not shown). Two FVB/N mice that remained persistently infected on day 115 p.i. had glucose levels of 10.4 and 10.8 mM/liters and hemoglobin values of 124 and 141 g/liter. In comparison, two mice that cleared the infection had glucose values of 9.7 and 10.4 mM/liter and hemoglobin values of 161 and 157 g/liter. The similarities in these results suggest that long-term persistence did not affect glucose or hemoglobin values.

Bacteria were consistently found in the cecum and, occasionally, also in single PPs of the terminal ileum in both BALB/c and FVB/N mice; bacterial counts in the ceca of infected, asymptomatic mice were similar in the different strains, varying between 9×10^4 and 1.3×10^6. Bacteria were found in the feces of infected, asymptomatic BALB/c and FVB/N mice throughout the infection period. The bacterial counts were between 10^3 and 10^6 CFU/g feces (see Table S1 in the supplemental material), which are similar to those found during acute infection (data not shown). Fecal pellets from mice that had cleared the infection (as shown by the lack of a bioluminescent signal for at least 3 days) did not contain any *Y. pseudotuberculosis*. These results suggest that the bacteria reside and multiply in a protected niche from where they are shed.

In summary, low-dose infections of *Y. pseudotuberculosis* result in persistent, asymptomatic infections in both FVB/N and BALB/c mice, where the bacteria mainly colonize the cecum from where they are shed. FVB/N mice maintain bacteria in the cecum for the longest time and appear as the most suitable model in which to study bacterial persistence.

***Yersinia* is present in the dome area of cecal patches surrounded by polymorphonuclear neutrophils (PMNs) during persistence.** The distinct spots of bioluminescent signals seen in infected ceca (Fig. 2B), together with the relatively large amounts of cultivable bacteria that could be isolated from these organs (see Table S1 in the supplemental material) and the observed shedding of bacteria during persistency, support the hypothesis of a protected niche for the bacteria. To investigate this further, infected ceca were sectioned and analyzed by immunofluorescence and histochemistry. The tissue sections that were chosen were at the location of the bioluminescent signals in the cecum. *Y. pseudotuberculosis* was detected by immunofluorescence, and rod-shaped bacteria were seen in close proximity to cecal lymphoid aggregates (or cecal patches), as single or, sometimes, multiple foci, mostly in the dome area facing the cecal lumen (Fig. 5A to C).

To examine whether bacterial colonization correlated with disease pathology, sections of cecal tissue were stained with toluidine blue to reveal the basic architecture of the tissue, as well as the localization of bacteria (Fig. 5D to F). The epithelium covering the cecal patch containing bacteria appeared disrupted in all analyzed samples ($n = 6$, days 24 to 35 p.i.), with lesions in the epithelium, and bacteria, together with cells, sloughed off into the lumen (exemplified in Fig. 5D). Immunohistochemistry showed typical B and T cell areas of a lymphoid aggregate, with no apparent change in distribution compared to that in control tissue (Fig. 5G and H; also see Fig. S4A and B in the supplemental material). Similarly, the distribution of macrophages and dendritic cells did not appear severely altered (Fig. 5I and J; see also Fig. S4C and D). However, a marked influx of polymorphonuclear neutrophils (PMNs) surrounding the bacteria was already evident at day 3 p.i. (data not shown) and still obvious at 34 days p.i. (Fig. 5K and L). PMNs were also present with the bacteria in luminal exudates (Fig. 5E, F, K, and L), which also could be seen upon combined immunofluorescent and 4′,6-diamidino-2-phenylindole (DAPI) staining of bacteria, showing exudates containing cells with multilobular nuclei and *Y. pseudotuberculosis* (Fig. 5C); hence, PMNs were the dominating immune cells that surrounded the bacterial foci.

***Y. pseudotuberculosis* persistency is associated with elevated serum levels of cytokines.** Given the presence of PMNs in the cecum during persistence, indicating an active immune response, we next investigated if the infection in asymptomatic mice affected cytokine levels in the animal. To analyze cytokine expression, serum was sampled from FVB/N mice infected with 10^7 CFU/ml, at days 1, 3, 7, 21, 29, 36, and 42 p.i., and analyzed using a multiplex array of 11 cytokines (IL-1β, IL-4, IL-10, IL-12p70, IL-15, IL-17, IL-18, IL-23, IFN-γ, KC, and TNF-α). Sera sampled from uninfected controls were analyzed in parallel.

Elevated levels of IL-1β, IL-4, IL-17, KC, and TNF-α were detected in sera from persistent mice at days 21 to 42 p.i. (Fig. 6). Levels of IL-10, IL-12p70, IL-15, IL-18, IL-23, and IFN-γ were similar to those in control samples at these later time points (see Fig. S5 in the supplemental material). Among the cytokines increased during persistence, KC already increased in the serum from day 1 p.i. and continued to also be high during persistent infection but decreased in mice that cleared the infection at days 36 and 42 p.i. (Fig. 6); thus, this result suggests the engagement of PMNs during the entire period of bacterial persistence. The increased serum levels of IL-1β, IL-4, IL-17, KC, and TNF-α during persistence likely reflect an ongoing complex host response involving Th2, Th1, and Th17 cells; PMNs; activated macrophages; and dendritic cells.

DISCUSSION

The acute infection model in mice has been widely used to study many important aspects of the enteric pathogen *Y. pseudotuberculosis*, such as its pathogenesis and host responses at different sites. However, this model has certain limitations, as the infection results in spread of bacteria to the liver and spleen, eventually causing mice to succumb to infection. Infection in humans begins in the intestine and spreads to the MLNs, causing clinical signs of acute enteritis, but the infection is usually self-limiting and resolved in immunocompetent persons, while systemic spread of the infection is mainly seen in immunocompromised individuals (5). Although one should not directly compare the host response in the mouse with the situation in an infected human, a mouse infection model where the infection results in resolution or persistence instead of systemic spread should be a more relevant model for studies of the host response to this pathogen.

Here, we have established a mouse model for studies of persistent infection of *Y. pseudotuberculosis* by using a sublethal infection dose. The presence of bacteria was detected using BLI of luminescent bacteria in real time in mice under anesthesia. BLI was proven excellent for analysis of bacterial colonization of *Y. pseudotuberculosis* infection *in vivo*, and progressive infections were distinguished from those that were resolved. This novel model allows studies of both host response and bacterial adaptation during prolonged and silent bacterial infections. This is important since incomplete clearance of bacterial infections may result in chronic disease. Moreover, there is considerably less known regarding the role of immune response as well as bacterial mechanisms involved in chronic compared with acute infections.

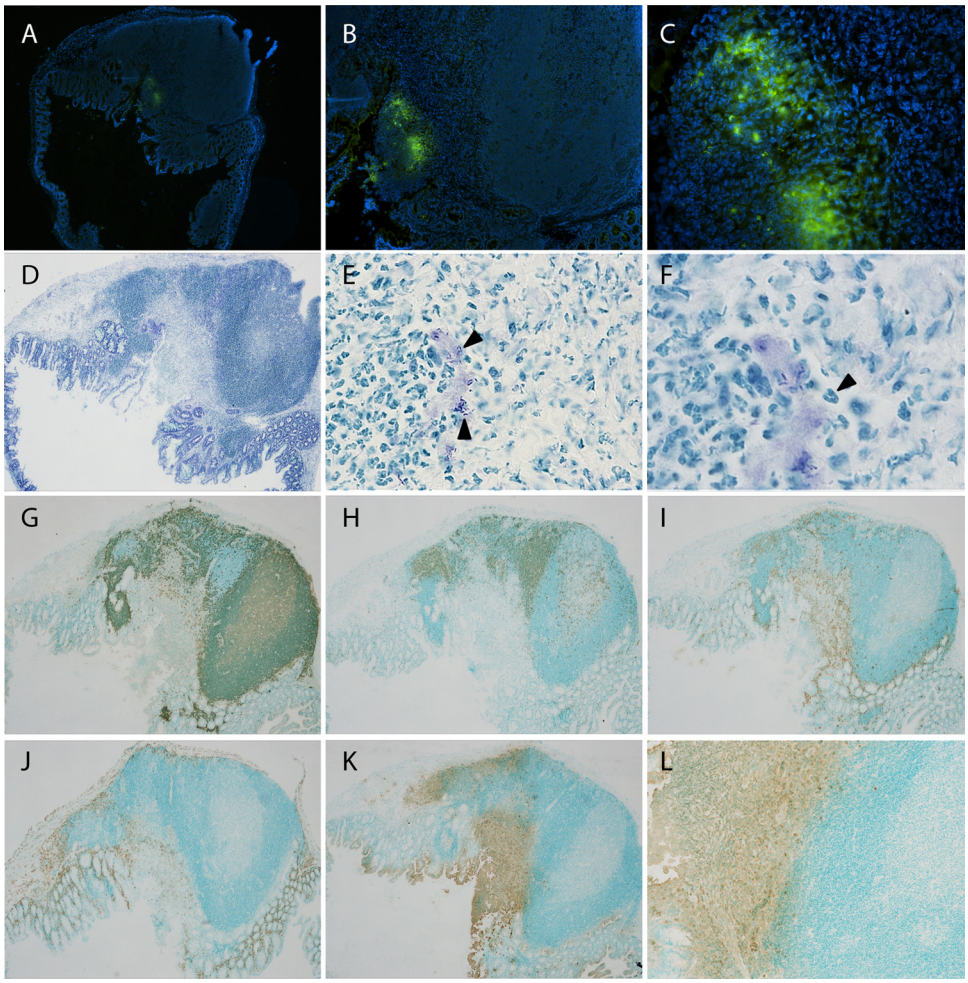

FIG 5 Characterization of cecal aggregates colonized by *Y. pseudotuberculosis*. Cecal tissues from mice positive for bioluminescent signals at day 34 postinfection were sectioned and analyzed by immunofluorescence and immunohistochemistry. (A to C) Immunofluorescent staining using anti-*Yersinia* polyclonal serum, detected by anti-rabbit-Al488 (green). Nuclei were stained with DAPI (blue). Magnifications: ×4 (A), ×10 (B), and ×40 (C). (D to F) Toluidine blue-stained sections. Magnifications: ×4 (D), ×60 (E), and ×100 (F). Arrowheads in panel E indicate bacteria, and that in panel F indicates a polymorphonuclear cell. (G to L) Immunohistochemical staining using monoclonal antibodies with amplification of signal by streptavidin-biotin and horseradish peroxidase-conjugated antibiotin: anti-B220 for B cells (G), anti-CD3 for T cells (H), anti-CD11c for dendritic cells (I), anti-F4/80 for macrophages (J), and anti-Ly6G/6C for PMNs (K and L). Positive cells are brown (diaminobenzidine), and the background is green (methyl green). Magnifications: ×4 (G to K) and ×10 (L). The stainings shown are representative from 6 individual persistent infected ceca.

We detected bacteria in mice that appeared totally asymptomatic and showed that the bacteria were contained in a localized area in the gut for an extended time. BLI of dissected organs from these mice revealed that bacteria were localized to the cecum in the majority of animals and, more specifically, to one or several cecal patches. Independent of the mouse strain that received a low inoculating dose, the cecum was the organ colonized initially and is also the organ where the bacteria were detected last; thus, it is likely the organ that is colonized until clearance. These results suggest that the cecum plays a pivotal role in *Yersinia* pathogenesis.

The finding that *Yersinia* localizes to the cecum early upon infection of mice is not at all new but has been seen previously upon infection with high doses, where the cecum is initially infected, as well as PPs of the small intestine (23, 24, 27). We suggest that the cecum is the main organ which is infected initially when low doses are used and that it may be the preferred site for infection. Infection of PPs would then be a consequence of a higher infection dose. There are several possible reasons why *Yersinia* is harbored in the cecum during persistence: the slower pace for intestinal content in the cecum than in the small intestine; the pocket shape of the cecum, which may allow bacteria to avoid the forces of movement of fecal matter through the intestine; the composition of the cecal microbiota; and surrounding nutrients shaped by the host and the local microbiota. Interestingly, persistent colonization in cecum for 100 days was recently reported to occur in mice infected by *Chlamydia muridarum* via the oral route, and without causing pathology (28).

Of the three mouse strains that were compared for low-dose infections with *Yersinia*, FVB/N proved to be the most susceptible strain for development of persistent infection, followed by BALB/c and then C57BL/6, which cleared the infection efficiently. BALB/c is considered to be more susceptible than C57BL/6 to enteric *Yersinia* infection (29, 30), likely reflecting the difference

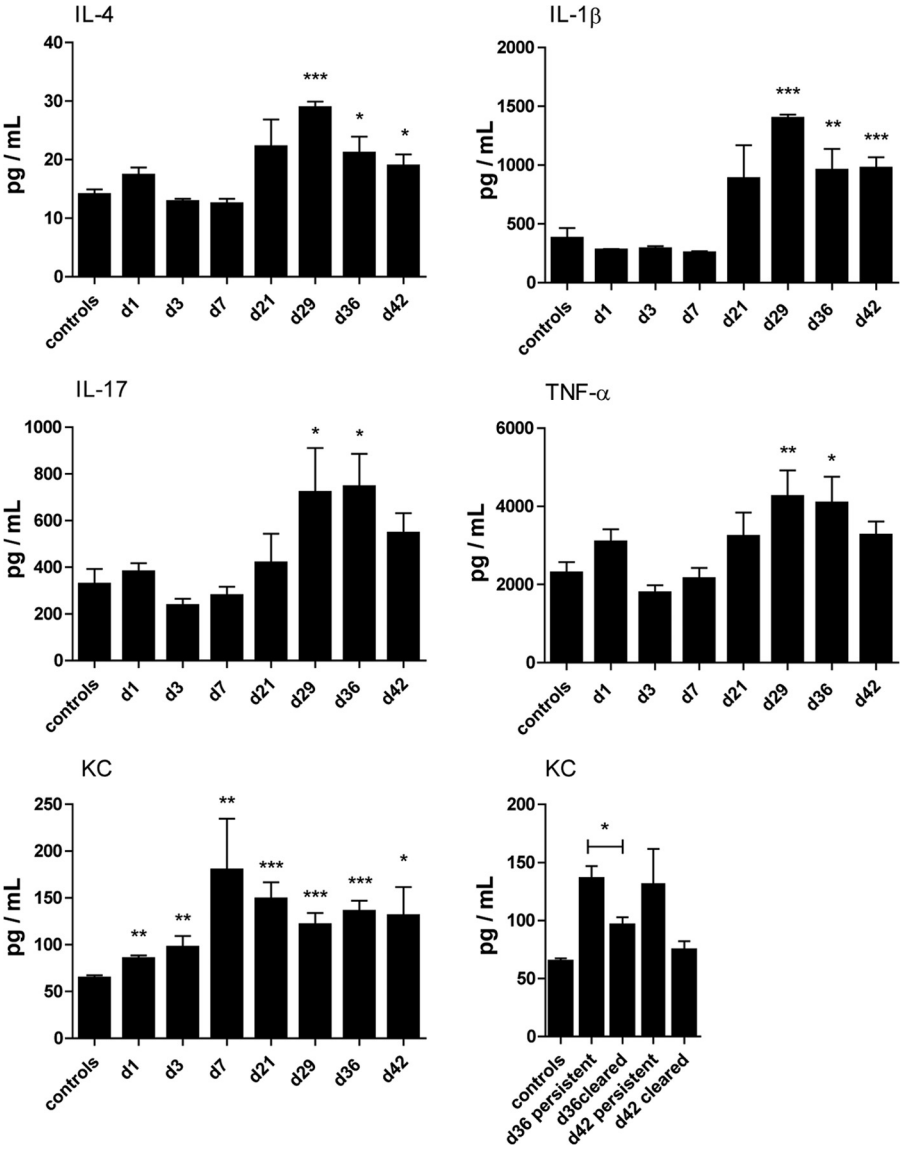

FIG 6 Cytokine profiles are altered in the serum from mice with persistent infections. Serum from infected FVB/N mice was sampled and analyzed by multiplex array for IL-4, IL-1β, IL-17, TNF-α, and KC on day 1 ($n = 5$), day 3 ($n = 5$), day 7 ($n = 6$), day 21 ($n = 8$), day 29 ($n = 5$), day 36 ($n = 10$ persistent), and day 42 ($n = 7$ persistent). Levels of KC in sera from infected mice are compared with levels in samples from mice that cleared infection on days 13 to 29 (day 36, $n = 9$; day 42, $n = 5$). The levels of analyzed cytokines in control serum were unchanged through the infection period and therefore were combined. Controls ($n = 2$) from each time point were grouped together. Data are presented as means ± standard errors of the means. Differences between controls and the respective analysis day were analyzed by unpaired *t* tests, with significance set at $P < 0.05$ (*), $P < 0.01$ (**), and $P < 0.001$ (***).

in the types of T cell immunity to which the different strains are more prone. Consistent with our data, a previous study which compared infections with *Y. enterocolitica* in BALB/c and C57BL/6 mice showed that C57BL/6 mice cleared the infection much more efficiently than did BALB/c mice (31). FVB/N mice have not been used for enteric *Yersinia* infections, with the exception of a study where *Nod2* knockout FVB/N mice were compared with wt FVB/N mice, using high doses for infection (32).

Different susceptibilities of mouse strains to infection have also been observed for other pathogens, including pneumococci (33). There are likely many underlying reasons why different mouse strains are more or less susceptible to infections by a certain pathogen, but one difference between the three strains used in the present study is in major histocompatibility complex (MHC) class I haplotypes, where the most resistant strain, C57BL/6, is H-2^b; the more susceptible BALB/c is H-2^d; and FVB/N is H-2^q. FVB/N mice are susceptible to persistent infection with murine encephalomyelitis virus, but FVB/N mice carrying an H-2^b transgene are more resistant, suggesting that the differences in MHC haplotypes play an important role in the susceptibility of different mouse strains to infectious agents (34).

Histochemical analysis revealed that cecal aggregates were colonized by bacteria during persistence and that the tissue was heavily infiltrated by PMNs. The epithelium was disrupted, and both bacteria and PMNs could be seen in luminal exudates that were released from the tissue. This shedding is an indication of ongoing

infection, but further analyses are required to understand the role of bacterial shedding during persistence. Given the presence of PMNs around bacterial foci in the cecal aggregates and the previously demonstrated importance of YopH and YopE for the antiphagocytic capacity of *Y. pseudotuberculosis* against PMNs (20, 35, 36), it was not surprising that these effectors together were found to be important for initial establishment of infection, which is a prerequisite for the development of persistent infection. Further, by using universal markers, we could not reveal any obvious effects on T cells, B cells, macrophages, and dendritic cells during the persistent state. However, cell subtypes could well be affected in numbers or by other means, and these studies are ongoing.

As infection in the cecal tissue was certain, an effect of cytokine profiles could be expected. Using a multiplex approach to measure cytokines in the blood of infected mice, we found that KC was elevated on days 7 to 21 and that IL-1β, IL-4, IL-17, and TNF-α were elevated on days 21 to 36 p.i. in sera of persistently infected mice. Moreover, most cytokines analyzed appeared to be high on day 1 p.i., reflecting a cytokine storm in the early stage of infection, which has also been observed for *Y. enterocolitica* infections (37). We were surprised that an effect of persistent infection could be seen in the blood of asymptomatic mice given the very low numbers of bacteria present in the cecum (10^6 to 10^7 CFU). However, as cytokine levels in the serum do not necessarily represent the true picture of what is going on in the intestinal compartment, a more detailed analysis of cytokine levels in the cecum is necessary to understand the local response. A systemic effect of cytokine responses could also indicate circulating antigens during persistent infection. Although highly speculative, this observation is interesting with regard to the hypothesis that development of *Yersinia*-associated reactive arthritis is a consequence of circulating antigens (38).

Our finding that a fraction of FVB/N and BALB/c mice develop an asymptomatic carrier state with bacteria residing in the cecum can have many important implications. This novel mouse infection model has great potential to unveil new knowledge of both bacterial adaptation and host immune defense mechanisms during persistent infection. There are multiple reports of asymptomatic intestinal carriage in pigs (39–41) and rodents (42). In these animals, bacteria localize to the cecum and are shed into feces, suggesting that bacteria reside in the cecum as a persistent infection, possibly as a natural reservoir that allows spreading in nature by shedding in feces (39). Interestingly, as a niche for bacterial infection in humans, the cecum has been reported as a site for infections by *Yersinia*, *Salmonella*, and *Campylobacter*, which all specifically infect the ileocecal area (43), suggesting that the organ is also a specifically beneficial habitat for these pathogens in humans. It remains unknown why some people develop a chronic carrier state whereas others do not. Long-term, chronic carriage of bacteria in humans has been related to other diseases (17, 44, 45), but robust data are still missing, with the exception of the link between *Y. pseudotuberculosis* and reactive arthritis (46).

ACKNOWLEDGMENTS

This work was supported by grants from the Swedish Research Council VR-M (K2014-56X-11222-20-5; M.F.); Insamlingsstiftelsen, Medical Faculty, Umeå University (M.F. and A.F.); and the Magnus Bergvalls Foundation (A.F.).

We thank Kristina Nilsson for outstanding technical assistance.

REFERENCES

1. **Rhen M, Eriksson S, Clements M, Bergstrom S, Normark SJ.** 2003. The basis of persistent bacterial infections. Trends Microbiol. **11:**80–86. http://dx.doi.org/10.1016/S0966-842X(02)00038-0.
2. **Monack DM, Mueller A, Falkow S.** 2004. Persistent bacterial infections: the interface of the pathogen and the host immune system. Nat. Rev. Microbiol. **2:**747–765. http://dx.doi.org/10.1038/nrmicro955.
3. **Grant SS, Hung DT.** 2013. Persistent bacterial infections, antibiotic tolerance, and the oxidative stress response. Virulence **4:**273–283. http://dx.doi.org/10.4161/viru.23987.
4. **Marteau P, Chaput U.** 2011. Bacteria as trigger for chronic gastrointestinal disorders. Dig. Dis. **29:**166–171. http://dx.doi.org/10.1159/000323879.
5. **Galindo CL, Rosenzweig JA, Kirtley ML, Chopra AK.** 2011. Pathogenesis of Y. enterocolitica and Y. pseudotuberculosis in human yersiniosis. J. Pathog. **2011:**182051. http://dx.doi.org/10.4061/2011/182051.
6. **Zganjer M, Roic G, Cizmic A, Pajic A.** 2005. Infectious ileocecitis—appendicitis mimicking syndrome. Bratisl. Lek. Listy **106:**201–202.
7. **Hanski C, Kutschka U, Schmoranzer HP, Naumann M, Stallmach A, Hahn H, Menge H, Riecken EO.** 1989. Immunohistochemical and electron microscopic study of interaction of Yersinia enterocolitica serotype O8 with intestinal mucosa during experimental enteritis. Infect. Immun. **57:**673–678.
8. **Marra A, Isberg RR.** 1997. Invasin-dependent and invasin-independent pathways for translocation of Yersinia pseudotuberculosis across the Peyer's patch intestinal epithelium. Infect. Immun. **65:**3412–3421.
9. **Clark MA, Hirst BH, Jepson MA.** 1998. M-cell surface beta1 integrin expression and invasin-mediated targeting of Yersinia pseudotuberculosis to mouse Peyer's patch M cells. Infect. Immun. **66:**1237–1243.
10. **Barnes PD, Bergman MA, Mecsas J, Isberg RR.** 2006. Yersinia pseudotuberculosis disseminates directly from a replicating bacterial pool in the intestine. J. Exp. Med. **203:**1591–1601. http://dx.doi.org/10.1084/jem.20060905.
11. **Galan JE, Wolf-Watz H.** 2006. Protein delivery into eukaryotic cells by type III secretion machines. Nature **444:**567–573. http://dx.doi.org/10.1038/nature05272.
12. **Durand EA, Maldonado-Arocho FJ, Castillo C, Walsh RL, Mecsas J.** 2010. The presence of professional phagocytes dictates the number of host cells targeted for Yop translocation during infection. Cell. Microbiol. **12:**1064–1082. http://dx.doi.org/10.1111/j.1462-5822.2010.01451.x.
13. **Cornelis GR.** 2002. The Yersinia Ysc-Yop 'type III' weaponry. Nat. Rev. Mol. Cell Biol. **3:**742–752. http://dx.doi.org/10.1038/nrm932.
14. **Heesemann J, Sing A, Trulzsch K.** 2006. Yersinia's stratagem: targeting innate and adaptive immune defense. Curr. Opin. Microbiol. **9:**55–61. http://dx.doi.org/10.1016/j.mib.2005.10.018.
15. **Viboud GI, Bliska JB.** 2005. Yersinia outer proteins: role in modulation of host cell signaling responses and pathogenesis. Annu. Rev. Microbiol. **59:**69–89. http://dx.doi.org/10.1146/annurev.micro.59.030804.121320.
16. **Girschick HJ, Guilherme L, Inman RD, Latsch K, Rihl M, Sherer Y, Shoenfeld Y, Zeidler H, Arienti S, Doria A.** 2008. Bacterial triggers and autoimmune rheumatic diseases. Clin. Exp. Rheumatol. **26:**S12–S17.
17. **Hoogkamp-Korstanje JA, de Koning J, Heesemann J.** 1988. Persistence of Yersinia enterocolitica in man. Infection **16:**81–85. http://dx.doi.org/10.1007/BF01644307.
18. **de Koning J, Heesemann J, Hoogkamp-Korstanje JA, Festen JJ, Houtman PM, van Oijen PL.** 1989. Yersinia in intestinal biopsy specimens from patients with seronegative spondyloarthropathy: correlation with specific serum IgA antibodies. J. Infect. Dis. **159:**109–112. http://dx.doi.org/10.1093/infdis/159.1.109.
19. **Ternhag A, Torner A, Svensson A, Ekdahl K, Giesecke J.** 2008. Short- and long-term effects of bacterial gastrointestinal infections. Emerg. Infect. Dis. **14:**143–148. http://dx.doi.org/10.3201/eid1401.070524.
20. **Westermark L, Fahlgren A, Fallman M.** 30 December 2013. Yersinia pseudotuberculosis efficiently escapes polymorphonuclear neutrophils during early infection. Infect. Immun. http://dx.doi.org/10.1128/IAI.01634-13.
21. **Isaksson EL, Aili M, Fahlgren A, Carlsson SE, Rosqvist R, Wolf-Watz H.** 2009. The membrane localization domain is required for intracellular localization and autoregulation of YopE in Yersinia pseudotuberculosis. Infect. Immun. **77:**4740–4749. http://dx.doi.org/10.1128/IAI.00333-09.
22. **Piwnica-Worms D, Schuster DP, Garbow JR.** 2004. Molecular imaging

of host-pathogen interactions in intact small animals. Cell. Microbiol. **6:**319–331. http://dx.doi.org/10.1111/j.1462-5822.2004.00379.x.
23. **Mecsas J, Bilis I, Falkow S.** 2001. Identification of attenuated Yersinia pseudotuberculosis strains and characterization of an orogastric infection in BALB/c mice on day 5 postinfection by signature-tagged mutagenesis. Infect. Immun. **69:**2779–2787. http://dx.doi.org/10.1128/IAI.67.5.2779-2787.2001.
24. **Logsdon LK, Mecsas J.** 2003. Requirement of the Yersinia pseudotuberculosis effectors YopH and YopE in colonization and persistence in intestinal and lymph tissues. Infect. Immun. **71:**4595–4607. http://dx.doi.org/10.1128/IAI.71.8.4595-4607.2003.
25. **Monack DM, Mecsas J, Ghori N, Falkow S.** 1997. Yersinia signals macrophages to undergo apoptosis and YopJ is necessary for this cell death. Proc. Natl. Acad. Sci. U. S. A. **94:**10385–10390. http://dx.doi.org/10.1073/pnas.94.19.10385.
26. **Meinzer U, Barreau F, Esmiol-Welterlin S, Jung C, Villard C, Leger T, Ben-Mkaddem S, Berrebi D, Dussaillant M, Alnabhani Z, Roy M, Bonacorsi S, Wolf-Watz H, Perroy J, Ollendorff V, Hugot JP.** 2012. Yersinia pseudotuberculosis effector YopJ subverts the Nod2/RICK/TAK1 pathway and activates caspase-1 to induce intestinal barrier dysfunction. Cell Host Microbe **11:**337–351. http://dx.doi.org/10.1016/j.chom.2012.02.009.
27. **Carter PB.** 1975. Animal model of human disease. Yersinia enteritis. Animal model: oral Yersinia enterocolitica infection of mice. Am. J. Pathol. **81:**703–706.
28. **Yeruva L, Spencer N, Bowlin AK, Wang Y, Rank RG.** 2013. Chlamydial infection of the gastrointestinal tract: a reservoir for persistent infection. Pathog. Dis. **68:**88–95. http://dx.doi.org/10.1111/2049-632X.12052.
29. **Hancock GE, Schaedler RW, MacDonald TT.** 1986. Yersinia enterocolitica infection in resistant and susceptible strains of mice. Infect. Immun. **53:**26–31.
30. **Autenrieth IB, Beer M, Bohn E, Kaufmann SH, Heesemann J.** 1994. Immune responses to Yersinia enterocolitica in susceptible BALB/c and resistant C57BL/6 mice: an essential role for gamma interferon. Infect. Immun. **62:**2590–2599.
31. **Schippers A, Mateika S, Prochnow B, Gruber AD, Muller W, Frischmann U.** 2008. Susceptibility of four inbred mouse strains to a low-pathogenic isolate of Yersinia enterocolitica. Mamm. Genome **19:**279–291. http://dx.doi.org/10.1007/s00335-008-9105-1.
32. **Meinzer U, Esmiol-Welterlin S, Barreau F, Berrebi D, Dussaillant M, Bonacorsi S, Chareyre F, Niwa-Kawakita M, Alberti C, Sterkers G, Villard C, Lesuffleur T, Peuchmaur M, Karin M, Eckmann L, Giovannini M, Ollendorff V, Wolf-Watz H, Hugot JP.** 2008. Nod2 mediates susceptibility to Yersinia pseudotuberculosis in mice. PLoS One **3:**e2769. http://dx.doi.org/10.1371/journal.pone.0002769.
33. **Kadioglu A, Andrew PW.** 2005. Susceptibility and resistance to pneumococcal disease in mice. Brief. Funct. Genomic. Proteomic. **4:**241–247. http://dx.doi.org/10.1093/bfgp/4.3.241.
34. **Azoulay-Cayla A, Syan S, Brahic M, Bureau JF.** 2001. Roles of the H-2D(b) and H-K(b) genes in resistance to persistent Theiler's murine encephalomyelitis virus infection of the central nervous system. J. Gen. Virol. **82:**1043–1047.
35. **Andersson K, Magnusson KE, Majeed M, Stendahl O, Fallman M.** 1999. Yersinia pseudotuberculosis-induced calcium signaling in neutrophils is blocked by the virulence effector YopH. Infect. Immun. **67:**2567–2574.
36. **Fahlgren A, Westermark L, Akopyan K, Fallman M.** 2009. Cell type-specific effects of Yersinia pseudotuberculosis virulence effectors. Cell. Microbiol. **11:**1750–1767. http://dx.doi.org/10.1111/j.1462-5822.2009.01365.x.
37. **Wang X, Gu W, Qiu H, Xia S, Zheng H, Xiao Y, Liang J, Jing H.** 2013. Comparison of the cytokine immune response to pathogenic Yersinia enterocolitica bioserotype 1B/O:8 and 2/O:9 in susceptible BALB/C and resistant C57BL/6 mice. Mol. Immunol. **55:**365–371. http://dx.doi.org/10.1016/j.molimm.2013.03.017.
38. **Toivanen A, Toivanen P.** 2000. Reactive arthritis. Curr. Opin. Rheumatol. **12:**300–305. http://dx.doi.org/10.1097/00002281-200007000-00012.
39. **Mair NS, Fox E, Thal E.** 1979. Biochemical, pathogenicity and toxicity studies of type III strains of Yersinia pseudotuberculosis isolated from the cecal contents of pigs. Contrib. Microbiol. Immunol. **5:**359–365.
40. **Fredriksson-Ahomaa M, Stolle A, Siitonen A, Korkeala H.** 2006. Sporadic human Yersinia enterocolitica infections caused by bioserotype 4/O:3 originate mainly from pigs. J. Med. Microbiol. **55:**747–749. http://dx.doi.org/10.1099/jmm.0.46523-0.
41. **Bonardi S, Paris A, Bassi L, Salmi F, Bacci C, Riboldi E, Boni E, D'Incau M, Tagliabue S, Brindani F.** 2010. Detection, semiquantitative enumeration, and antimicrobial susceptibility of Yersinia enterocolitica in pork and chicken meats in Italy. J. Food Prot. **73:**1785–1792.
42. **Backhans A, Fellstrom C, Lambertz ST.** 2011. Occurrence of pathogenic Yersinia enterocolitica and Yersinia pseudotuberculosis in small wild rodents. Epidemiol. Infect. **139:**1230–1238. http://dx.doi.org/10.1017/S0950268810002463.
43. **Puylaert JB, Van der Zant FM, Mutsaers JA.** 1997. Infectious ileocecitis caused by Yersinia, Campylobacter, and Salmonella: clinical, radiological and US findings. Eur. Radiol. **7:**3–9. http://dx.doi.org/10.1007/s003300050098.
44. **Watson GT, Huaman MA, Semler MW, Manners J, Woron AM, Carpenter LR, Christman BW.** 2013. When nature meets nurture: persistent Yersinia infection. Am. J. Med. **126:**578–580. http://dx.doi.org/10.1016/j.amjmed.2013.03.006.
45. **Netea MG, van der Leij F, Drenth JP, Joosten LA, te Morsche R, Verweij P, de Jong D, Kullberg BJ, van der Meer JW.** 2010. Chronic yersiniosis due to defects in the TLR5 and NOD2 recognition pathways. Neth. J. Med. **68:**310–315.
46. **Hannu T, Mattila L, Nuorti JP, Ruutu P, Mikkola J, Siitonen A, Leirisalo-Repo M.** 2003. Reactive arthritis after an outbreak of Yersinia pseudotuberculosis serotype O:3 infection. Ann. Rheum. Dis. **62:**866–869. http://dx.doi.org/10.1136/ard.62.9.866.